Journal of Food Chemistry & Nanotechnology

https://doi.org/10.17756/jfcn.2022-140

Research Article

Open Access

Morula Leaf Extract Mediated Synthesis of Silver Nanoparticles and their Application in the Analysis of SCN− Based on Inhibition of the Nanozyme Activity on 3,3′,5,5′-Tetramethylbenzidine (TMB) by the Silver Nanoparticles

Oratile Semong* **and Bareki Shima Batlokwa**

Department of Chemical and Forensic Sciences; College of Science; Botswana International University of Science and Technology, Palapye, Botswana, Southern Africa

***Correspondence to:**
Oratile Semong
Department of Chemical and Forensic Sciences; College of Science; Botswana International University of Science and Technology, Palapye, Botswana, Southern Africa
Email: mogapaesio@biust.ac.bw

Received: October 17, 2022
Accepted: December 22, 2022
Published: December 24, 2022

Citation: Semong O, Batlokwa BS. 2022. Morula Leaf Extract Mediated Synthesis of Silver Nanoparticles and their Application in the Analysis of SCN− Based on Inhibition of the Nanozyme Activity on 3,3',5,5'-Tetramethylbenzidine (TMB) by the Silver Nanoparticles. *J Food Chem Nanotechnol* 8(4): 192-200.

Copyright: © 2022 Semong and Batlokwa. This is an Open Access article distributed under the terms of the Creative Commons Attribution 4.0 International License (CC-BY) (http://creativecommons.org/licenses/by/4.0/) which permits commercial use, including reproduction, adaptation, and distribution of the article provided the original author and source are credited.

Published by United Scientific Group

Abstract

The monitoring of thiocyanate (SCN^-) in food is of consumer health and safety relevance. In this work, a colorimetric method for the detection of SCN^- in milk using a silver nanoparticles (AgNPs) nanozyme is presented. Here, silver nanoparticles were synthesized using the leaf extracts of *Sclerocarya birrea* (marula). The nanoparticles exhibited intrinsic oxidase mimetic catalytic activity. They could efficiently catalyze the colorimetric oxidation of 3,3′,5,5′ - tetramethylbenzidine (TMB) in the presence of oxygen to form a blue colored cation radical with a characteristic absorption peak at 654 nm. We found out that adding thiocyanate (SCN^-) strongly inhibited this colorimetric reaction by decreasing the oxidase-like activity of the AgNPs selectively. The inhibition and color variation of the assay was proportional to the concentration of SCN^-. Based on these findings a colorimetric assay for the detection of SCN^- was established. The assay exhibited excellent selectivity against potential interferents and sensitivity with a low detection limit of 2.89 μM. This novel application showed high accuracy with excellent recoveries of between 89.4 and 118.1 %, along with fast detection times of 3 min employing low sample volumes. These excellent characteristics of the developed assay present it as a potential simple, fast, sensitive, selective, visual, equipment free point-of-need diagnostic tool of high throughput for food safety diagnosis.

Keywords

Thiocyanate, Colorimetry, *Sclerocarya birrea* (Marula), Silver nanoparticles, Oxidase-like activity, nanozymes

Abbreviations

SCN^-: Thiocyanate ion; **TMB**: 3,3′,5,5′- tetramethylbenzidine; **AgNPs**: silver nanoparticles; **LPS**: lactoperoxidase system; **XRD**: x-ray diffraction; **SEM**: Scanning electron microscope; **V_{max}**: maximal reaction velocity; **k_m**: Michaelis- Menten constant; **H_2O_2**: hydrogen peroxide; **$AgNO_3$**: Silver nitrate; **Au@Pt**: core-shell gold/platinum nanocatalysts; **Au QDs**: gold quantum dot; **GQDs-AuNP**: gold nanoparticles/graphene quantum dots hybrids; **PdCu**: bimetallic Palladium Copper naoppernocorals; **AgNP/FP**: silver nanoparticles coated filter paper; **SO_4^-**: Sulphate; **Cl^-**: chloride; **NO_3^-**: nitrate; **$S_2O_3^{2-}$**: sulphite; **K^+**: potassium ion; **Ca^{2+}**: calcium ion; **Fe^{3+}**: iron ion, **Mg^{3+}**: magnesium ion; **Zn^{2+}**: zinc ion, **Cs^+**: cesium ion; **Fe_3O_4**: iron oxide.

Introduction

Thiocyanate, its metabolic precursors and/its by-products are commonly found in food such as broccoli, kale, cabbage, lima beans, and sweet potatoes [1].

Moreover, it is found in milk as part of the lactoperoxidase system [2]. The lactoperoxidase system is a natural antibiotic system in milk [3]. The oxidation of halides and thiocyanate by hydrogen peroxide (H_2O_2), is facilitated by the lactoperoxidase enzyme in the production of a range of antimicrobial compounds [4]. In a series of reactions, thiocyanate is converted into hypothiocyanous acid (HOSCN). At the normal pH of milk, HOSCN is dissociated and exists mainly in the form of hypothiocyanate ions ($OSCN^-$) [5]. This agent reacts specifically with free sulphydryl groups (- SH), thereby inactivating several vital metabolic bacterial enzymes, consequently, blocking their metabolism and ability to multiply, therefore prolonging the shelf life of milk [6]. SCN^-'s inherent concentration in milk is about 5-8.5 mg/L [7]. To activate the lactoperoxidase system, 20 mg/L of thiocyanate is needed [8]. In countries where adequate refrigeration equipment is not accessible, and where it is permitted by regulation, the LPS may be artificially activated by augmenting the thiocyanate ion using sodium percarbonate or sodium thiocyanate to temporarily inhibit pathogenic microorganisms and increase storage stability of milk [9, 10]. When used as intended, thiocyanate treated milk is safe for consumption [2]. However, when added in excess, SCN^- can interfere with iodide uptake and may potentially disrupt synthesis of the thyroid hormone [11]. In addition, higher SCN^- concentrations in the human body lead to vertigo or unconsciousness [7]. Thus, to protect consumers, a regulatory levels of 14 mg/L SCN^- in milk has been set by the International Dairy Federation [6]. In India, activating the LPS by adding thiocyanate is not permitted by the food regulatory authorities [2] and in China, thiocyanate has been withdrawn as a food preservative since 2007 [3].

To ensure that set regulatory levels are adhered to, various techniques have been reported for the analysis of SCN^- in milk. These include spectrophotometric determination [12], high-performance liquid chromatography with fluorometric detection [13], voltammetry [14], ion chromatography with suppressed conductivity detection [15], capillary zone electrophoresis with a diode array detector [16], fluorescence [17] and Surface-Enhanced Raman Scattering (SERS) [11]. Although these techniques have the advantages of high accuracy and sensitivity, they are limited by expensive sophisticated instruments that require trained professional technicians, poor selectivity, low throughput and long operation times which limit their wide use in ordinary institution and routine detection [18, 19]. Thus, it is urgent to develop analytical tools and strategies that employ novel, smart functional materials that are easy to develop, cheap, sensitive and can assist in achieving rapid, easy to interpret, precise and accurate analysis or screening of SCN^- in milk especially at ports of entry for a landlocked country like Botswana that heavily relies on importation of milk. With the advantage of onsite analysis, visualization, simplicity, sensitivity, affordability, high throughput, and no requirement for skillful technicians, nanozymes have gained great attention as such smart functional materials.

Nanozymes are nanomaterials with intrinsic enzyme-like activities [20]. Yan et al. [21] first discovered Fe_3O_4 nanocrystals as peroxidase-mimics in 2007. Subsequently, several nanomaterials were investigated for possessing intrinsic biological enzyme-like activities predominantly catalytic activities similar to peroxidase, oxidase, catalase and superoxidase dismutase enzymes [22]. To the best of our knowledge only five nanozymes all possessing peroxidase-like activity have been developed for the colorimetric detection of SCN^-. These include core-shell Au@Pt nanocatalysts (Au@Pt) [23], gold quantum dots (Au QDs) [1], gold nanoparticles/graphene quantum dots hybrids (GQDs- AuNP) [19], bimetallic PdCu nanocorals (PdCu) [24] and silver nanoparticles decorated filter paper (AgNP/FP) [25]. In reactions involving peroxidase mimics, hydrogen peroxide is reduced, along with chromogenic substrates such as 3,3′,5,5′-tetramethylbenzidine (TMB), 2,2′-azino-bis-(3-ethylebenzothiozoline-6-sulphonic acid (ABTS) and o-phenylene diamine (OPD) being oxidized as electron donors to produce a color change [26]. In the presence of an analyte, the peroxidase-like activity of these nanozymes can either be enhanced or suppressed. The effect is concentration dependent and can be monitored chromogenically. From such reactions, assays for the colorimetric detection of SCN^- have been developed. However, such assays that use peroxidase mimics have shortcomings, the hydrogen peroxide (H_2O_2) used is destructive and unstable [27]. Furthermore, current available nanozymes for the detection of SCN^- have been prepared using toxic chemicals.

Hence, in this work a facile green method for the preparation of silver nanoparticles using *Sclerocarya birrea* (Marula) leaf extract and silver nitrate ($AgNO_3$) is presented. *Sclerocarya birrea* (marula) plant is an abundant plant in Botswana. The use of the plant extract offers a more rapid, sustainable, non-toxic, and eco-friendly option. The proposed silver nanoparticles nanozyme catalyzes the oxidation of TMB in the presence of oxygen as a green oxidant. We found out that adding SCN^- strongly inhibits the oxidase-like activity of the nanoparticles, such that the substrate molecules are only oxidized to a lesser extent and the sensing solution is light blue or even colorless. The color variation of the sensor is related to the concentration of SCN^-. Therefore, this strategy is used to quantitatively detect SCN^-. The excellent performance with regards to sensitivity, accuracy, selectivity and precision along with rapid detection and low sample volumes required for this novel application in food safety diagnosis are established.

Materials and Methods

Chemicals

The silver nitrate used for preparing the nanoparticles was purchased from Merck (Darmstadt, Germany). Cesium nitrate, lead (III) nitrate, ascorbic acid, L-lysine, cysteine, and glutathione were purchased from Sigma Aldrich (Johannesburg, South Africa). Aluminum nitrate nonahydrate and ferric chloride hexahydrate were purchased from Ace Chemicals (Johannesburg, South Africa). Fructose and glucose were purchased from Saarchem (Johannesburg, South Africa). Calcium chloride dihydrate, magnesium nitrate hexahydrate, potassium sulphate, sodium sulphite, and ferrous sulphate were supplied by Rochelle (Johannesburg, South Africa). Sodium nitrate, zinc nitrate, potassium thiocyanate, methanol, sodium phosphate dibasic hydrate, and citric acid were purchased from Merck (Darmstadt, Germany). The reagents in this work were

of analytical grade and were used without additional purification. All analyte solutions were prepared in Millipore ultrapure double deionized water.

Instrumentation

The morphology of the prepared AgNPs was observed using the Carl Zeiss Gemini SEM500 Electron microscope (Berlin, Germany). X-ray diffraction (XRD) patterns were obtained on an Empyrean x-ray diffractometer supplied by PANalytical (Malvern, United Kingdom) for a 2θ range of 20–80. The UV-vis spectra were collected using a Thermofisher UV-visible absorbance spectrophotometer (Waltham, MA, USA).

Synthesis of *Sclerocarya birrea* morula extract reduced silver nanoparticles

The silver nanoparticles were prepared from *Sclerocarya birrea* leaf extracts using a method by Nyoni et al. [28] with some modifications. Briefly, to remove impurities, fresh *Sclerocarya birrea* leaves were washed several times with deionized water. The leaves were air dried in the shade at room temperature. These were then ground into fine powder. 5 g of the dried leaves were boiled at 120 °C in 50 mL deionized water for about 5 min while stirring. The extract was cooled to 25 °C and filtered three times. For the preparation of the silver nanoparticles 150 µL of the extract was added to 100 mL, 5 mM $AgNO_3$ while stirring. The formation of nanoparticles was monitored every 15 min for 3 h using UV-vis spectrophotometer.

Evaluation of oxidase-like activity

The oxidase-like activity of the AgNPs and their significance in colorimetric detection of SCN^- was studied with TMB as a chromogenic substrate. Several reaction mixtures were prepared in citrate-phosphate buffer and UV/visible absorption spectroscopy measurements were carried out to determine the extent of TMB oxidation. These included, TMB alone; TMB and AgNPs; TMB and SCN^-; TMB, SCN^- and AgNPs. The substrate color change associated with different reaction systems was used to evaluate the oxidase-like activity of the AgNPs.

Optimization of parameters for the detection of thiocyanate

To achieve high efficiency in the detection of thiocyanate, a series of experiments were carried out to attain optimal parameters, such as volume of silver nanoparticles, concentration of TMB, incubation time and buffer pH. Typically, in a 2 mL eppendorf tube, 25 μL AgNPs was mixed with 50 μL of thiocyanate then 1000 μL of citrate-phosphate buffer was added and then finally 100 μL of TMB was added. The mixture was then incubated for 3 min. For the control, deionized water was used instead of thiocyanate. After incubation, absorbances were recorded at λmax = 654 nmto assess the catalytic activity of AgNPs. All the experiments were done in triplicates.

Evaluation of the performance of the AgNPs nanozyme

To evaluate the sensitivity of the AgNPs in the detection of SCN^-, under optimal conditions, SCN^- solutions of varying concentrations (0-1000 μM) were added to the detection system and incubated for 3 min. After incubation absorbances were recorded at λmax = 654 nm. To assess selectivity, some competing species were used instead of SCN^-. To expand the field of application, SCN^- was analyzed in the presence of the competing species at equal concentrations (100 μM).

Steady state Kinetics

Under optimal conditions, the steady-state kinetics of the AgNPs towards the oxidization of TMB with dissolved oxygen were studied. Here the absorbance intensities of varying concentrations of TMB (2.0 – 10.0 mM) in the presence of the AgNPs were measured at 1 min intervals for 5 min.

Results and Discussion

Synthesis of *Sclerocarya birrea* morula extract reduced silver nanoparticles

AgNPs were prepared by the method described. The silver nitrate solution color changed from clear to yellowish brown solution with time after the plant extract was added. This was confirmation of successful synthesis of AgNPs [29]. The surface plasmonic resonance (SPR) peak of the silver nanoparticles was observed at around 434 nm as shown on figure 1. The peak intensities for silver nanoparticles increased with increasing reaction time as indication of increasing concentration of AgNPs with time.

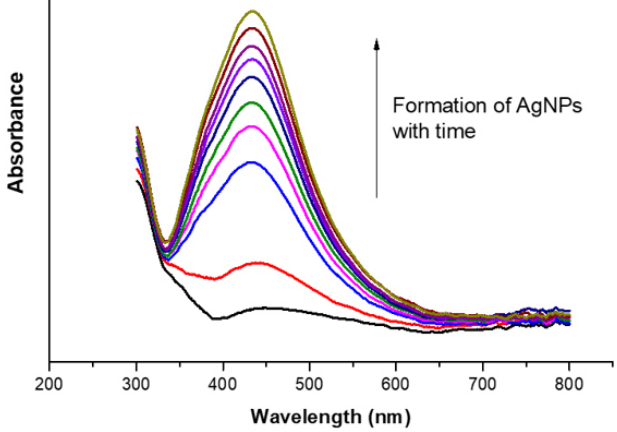


Figure 1: Biosynthesis of AgNPs; UV Spectra of AgNPs prepared using marula leaf extract and silver nitrate at different time intervals.

Characterization of the *Sclerocarya birrea* extract reduced AgNPs

The scanning electron micrograph on figure 2 shows spherical AgNPs. The micrograph shows bright AgNPs which were easy to identify due to contrasting backscattered light in SEM images of metals like silver which show higher secondary electron emission [30]. The crystalline nature of the AgNPs was confirmed by X-ray diffraction spectrometry (XRD) figure 3.The diffraction peaks at 37.54°, 46.94°, and 66.68° were indexed with planes (111), (200), and (220). The peak at 37.54° in the diffraction pattern, is said to indicate the successful materialization, and small crystal size of the AgNPs [31]. [30] reported a diffraction peak at 32.20° with plane (101) is characteristic in bio synthesized AgNPs. Similarly, a peak at

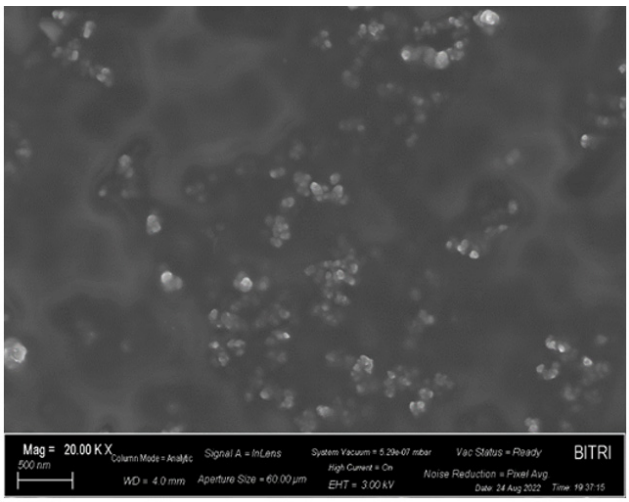


Figure 2: SEM micrograph of the synthesized AgNPs.

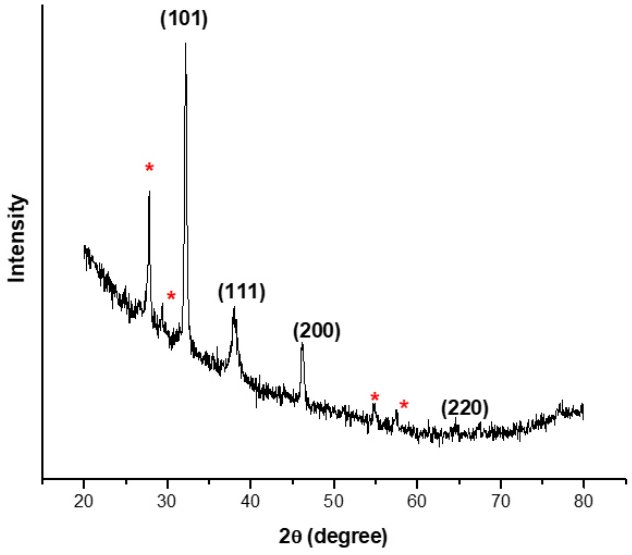


Figure 3: XRD spectrum of biosynthesized AgNPs.

32.19° indexed with plane (101) was present in our diffraction pattern. [32] attributed the peaks shown in asterisks to the presence of phytochemicals from the leaf extract. The obtained X-ray diffraction pattern matches well with those in literature [30-31] and thus clearly showed the successful preparation of AgNPs using marula leaf extract.

Oxidase mimetic activity of AgNPs on TMB and inhibition by SCN^-

The oxidase-like activity of AgNPs towards the oxidation of TMB and the effect of SCN^- on the reaction were studied. As can be seen on figure 4, AgNPs catalyzed the oxidation of TMB in the presence of dissolved oxygen, with the appearance of the characteristic absorbance peak of oxidized TMB (oxTMB) at 654 nm and the formation bright blue colored oxTMB. Here, the one-electron oxidation of TMB in solution produces a blue colored charge-transfer complex of the parent compound and its imine oxidation product in equilibrium with its cation free-radical [33]. However, when 100 µM SCN^- was added to the system a light blue oxTMB was formed with the absorbance peak being reduced by a factor of

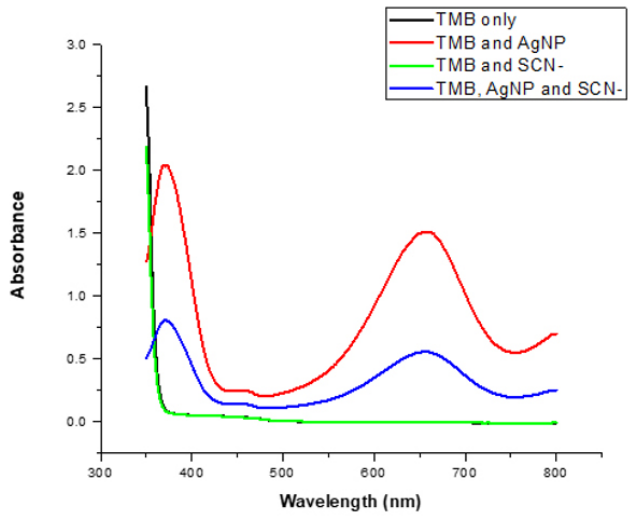


Figure 4: UV/Visible spectra of reaction systems containing TMB only, TMB and AgNP, TMB and SCN- and TMB, AgNP and SCN.

3. SCN^- inhibited the catalytic activity of the AgNPs on the oxidation of TMB. SCN^- is known to adsorb onto the surface of metal nanoparticles forming metal-S bonds [34, 35]. This has been said to block the active sites of such nanoparticles and hence inhibiting their catalytic property [25]. No observable color change was seen for TMB alone and TMB and SCN^- as can be seen by the flat absorbance graphs for the two reaction mixtures. This further confirms that the suppressed oxidation of TMB is due to interaction of SCN^- with the catalyst and not SCN^- with TMB.

Optimization of experimental conditions

Like natural enzymes, the catalytic activity AgNPs can be affected by concentration of the catalyst, pH, incubation time and concentration of the substrate. To obtain high sensitivity for SCN^- detection, some experimental conditions were optimized. The absorbance signal in the presence and absence of SCN^- were denoted A and A0 respectively and the difference in absorbance, ΔA in the presence and absence of SCN^-, ΔA=A0-A. Figure 5a shows increasing absorbance signal with increasing AgNPs amount.However, the effect of the presence of SCN^- was limited by excess AgNPs. Taking this into consideration 30 µL was selected as the optimal amount of AgNPs. At this point on the graph, A0-A was at its maximum.

Similarly, the concentration of TMB was optimized. In the absence of SCN^-, the absorbance intensity increased with increasing TMB concentration. This meant that at each concentration level of TMB, there was more TMB available to be oxidised and the catalyst had enough active sites to accommodate the TMB molecules, hence more oxTMB was formed. On the other hand, in the presence of SCN^-, TMB was oxidised to a lesser extent even with increasing concentration of TMB. This is depicted by lower absorbance intensities at the same TMB concentration on figure 5b and it is due to the inhibition of active sites on the nanozyme by SCN^-. The difference in absorbance intensities of oxTMB increased gradually with TMB concentration at lower levels until reaching a maximum at 8mM then flattened. Hence 8 mM was chosen as the optimal TMB concentration as it had the highest absorbance difference.

Incubation time was also assessed in the presence and absence of SCN^-. As shown on figure 5c, initially the absorbance increased rapidly signalling a fast reaction rate for the oxidation of TMB. Thereafter, the absorbance only increased insignificantly. This shows that from the start of the experiment there were a lot of active sites on the nanozyme available for the adsorption of TMB and O_2, however as the experiment progressed the active sites of the nanozyme became saturated such that the reaction rate was reduced hence the absorbance appear to be similar as the reaction progressed. The absorbance difference was maximum at 3 min therefore for further experiments 3 min was used as the optimal incubation time. The oxidation of TMB is said to be acid-dependent due to its limited solubility in aqueous solutions, which is improved in acid media due to the protonation of one of amino groups, hence the optimization of pH was done in acidic media (pH values 3.0-6.0). As seen figure 5d in the absence of SCN^-, at lower pH values the absorbance due to the oxidation of TMB is low. This is because at low pH values both the amino groups on the substrate are protonated, and this makes the substrate insusceptible to catalytic oxidation [36]. The absorbance was highest between pH values of 4.0 and 5.0. For TMB, maximum oxidation reaction efficiency is usually observed in a pH range of 4.0 to 5.0 [25] due to protonation of one of amino group. Our results agree with this. Furthermore, the absorbance was lowest at pH 4 in the oxidation of TMB in the presence of SCN^-, this means that SCN^- was able to suppress the catalytic activity of the nanozyme more efficiently at pH 4. A-A0 was maximum at pH 4, therefore this pH was used as the optimal pH.

Steady state kinetics

The steady-state kinetics for the oxidase-like activity of AgNPs towards the oxidization of TMB with dissolved oxygen were studied. Beer-lambert law was used to make an approximation of the initial catalytic rate. Here the slope of absorbance at 654 nm per unit time was taken as the initial rate for a given range of concentrations of TMB. From these,

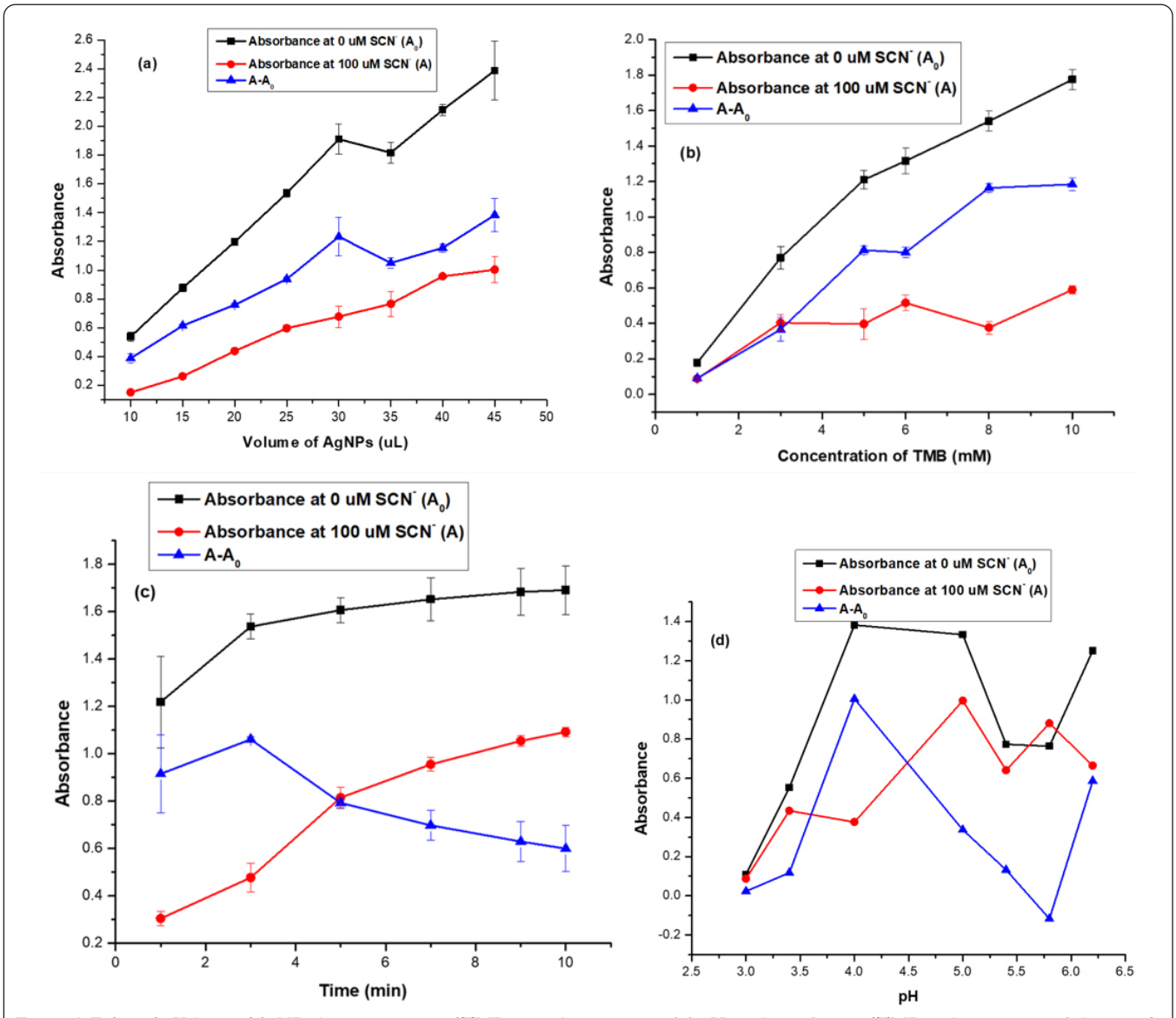


Figure 5: Effect of a.Volume of AgNPs, b. concentration of TMB, c. incubation time and d. pH on the oxidation of TMB in the presence and absence of SCN^-.

a typical Michaelis–Menten curve was obtained figure 6a and the Lineweaver-Burke curve figure 6b was plotted to obtain the maximal reaction velocity (V_{max}) and Michaelis–Menten constant (K_m). K_m was determined as 0.08461 mM. The low K_m value reflects the high affinity of the nanozyme towards the substrate, TMB. We found V_{max} of 7.10 µM/s. This high V_{max} value means that the nanozyme exhibited a high enzymatic activity towards TMB. K_m and V_{max} values of published work on nanozymes for the detection of SCN^- and AgNPs prepared in this study are given in table 1. The lower K_m value of AgNPs shows the stronger affinity of the AgNPs in this work towards TMB compared to other nanoparticles prepared for the detection of SCN^-.

Colorimetric detection of SCN–

Figure 7a shows UV-Vis spectra of inhibition of TMB oxidation at different SCN^- concentrations. At 654 nm the absorbance decreases with increasing SCN^- concentration. The relationship between absorbance and concentration of SCN^- is presented in figure 7b and from this the calibration curve in the range 2-50 µM is obtained (**insert**). The LOD of the colorimetric sensor is calculated using the equation, LOD = $3\sigma/k$, where k is the slope of the calibration curve, and σ is the standard deviation of the y-intercept. It was calculated to be 2.89 µM.

Effect of potentially interfering compounds

To assess the selectivity of the assay, several potential interferents were studied, including anions (SO_4^-, Cl^-, NO_3^-, $S_2O_3^{2-}$), metal ions (K^+, Ca^{2+}, Fe^{3+}, Mg^{3+}, Zn^{2+}, Cs^+), sugars (glucose, and fructose), amino acids (lysine, cysteine, glycine, and glutathione) and ascorbic acid, which may typically be present in milk. On figure 8a strike through SCN^- had the lowest absorbance intensity compared to potential interferants, this means that it has the great inhibitory effect on the catalytic activity of the AgNPs. Of the possible interferents analyzed only glutathione (which also contains the thiol group) seemed to considerably inhibit the catalytic activity of AgNPs although to a lesser extent compared to SCN^-. When SCN^- was analyzed in the presence of competing species figure 8b, its inhibitory effect was maintained although to a lesser when compared to when SCN^- was analyzed alone. These results have been analyzed on the bar graph on figure 8c.

Analysis of milk samples

To assess the validity of the colorimetric method in detecting SCN^- in real samples, milk samples were spiked with different amounts of SCN^-. The results presented on table 2 show that recoveries over the ranges 89.4-118.1 % were obtained. These results indicated that the proposed method is reliable and suitable for practical application.

Conclusion

In summary, we developed a colorimetric assay for the detection of SCN^- in milk, based on the suppressed oxidase-like activity of marula extract synthesized AgNPs. This colorimetric assay offered good selectivity, excellent sensitivity, favorable reliability, and accuracy. Furthermore, it was applied in the anal-

Table 1: Michaelis–Menten constant, km and maximum reaction rate, vmax of AgNPs and other nanozymes used for the detection of SCN^-.

Catalyst	Substrate	km (mM)	Vmax (M/s)	Reference
AgNP/FP	TMB	2.23	$2.873*10^{-7}$	[25]
Bimetallic PdCu	TMB	0.25	$1.19*10^{-8}$	[24]
Au QDs	TMB	0.38	-	[1]
AgNPs	TMB	0.085	$7.10*10^{-6}$	this work

Table 2: Determination of SCN- in real samples by UV-Vis (n=3).

Sample	Spiked (µM)	Detected (µM)	Recovery(%)
Milk	10.0	8.9 ± 2.4	89.4
	15.0	17.7 ± 4.2	118.1
	30.0	28.5 ± 1.4	95.1

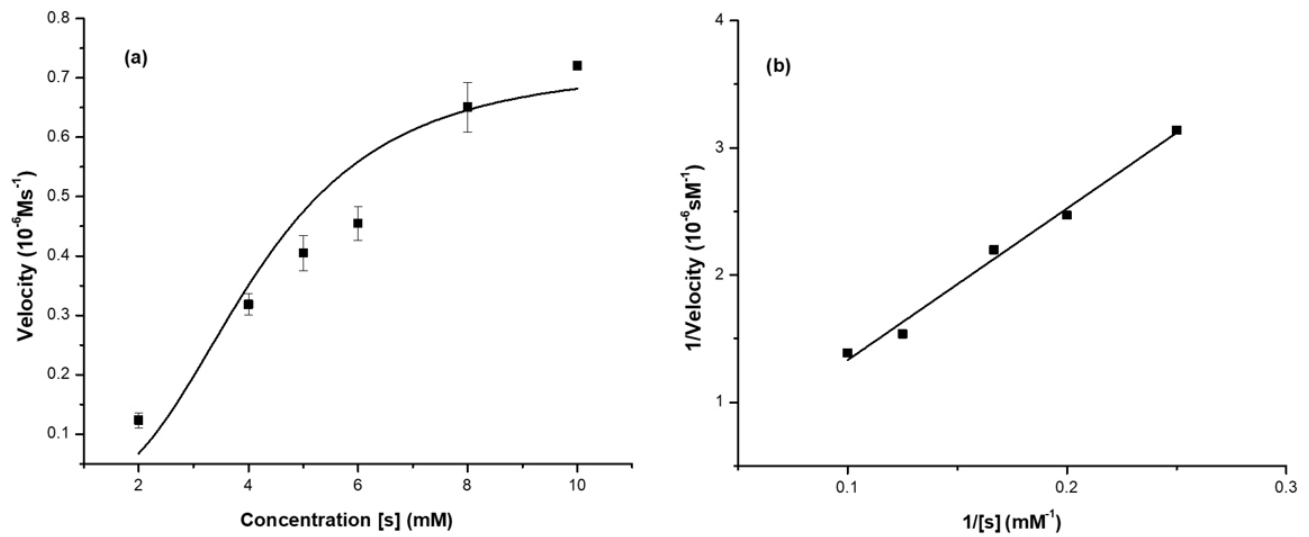


Figure 6: Steady state kinetics at varying TMB concentrations, Michaelis-Menten curve and the corresponding Lineweaver-Burke plot.

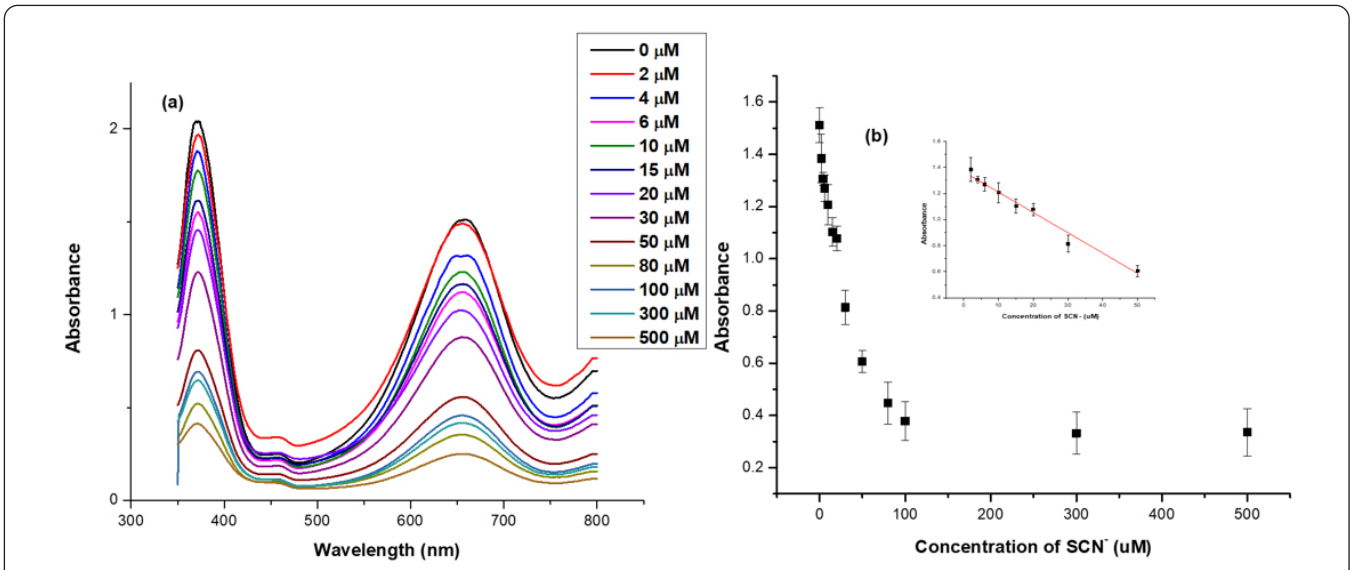


Figure 7. Sensitivity of AgNPs towards SCN^-. a. absorption spectra of TMB under varying concentrations of SCN^- (0-500 µM), b. plot of absorbance variation versus the concentration of SCN^- added (insert: linear relationship between Absorbance and concentration of SCN^- (n=3)

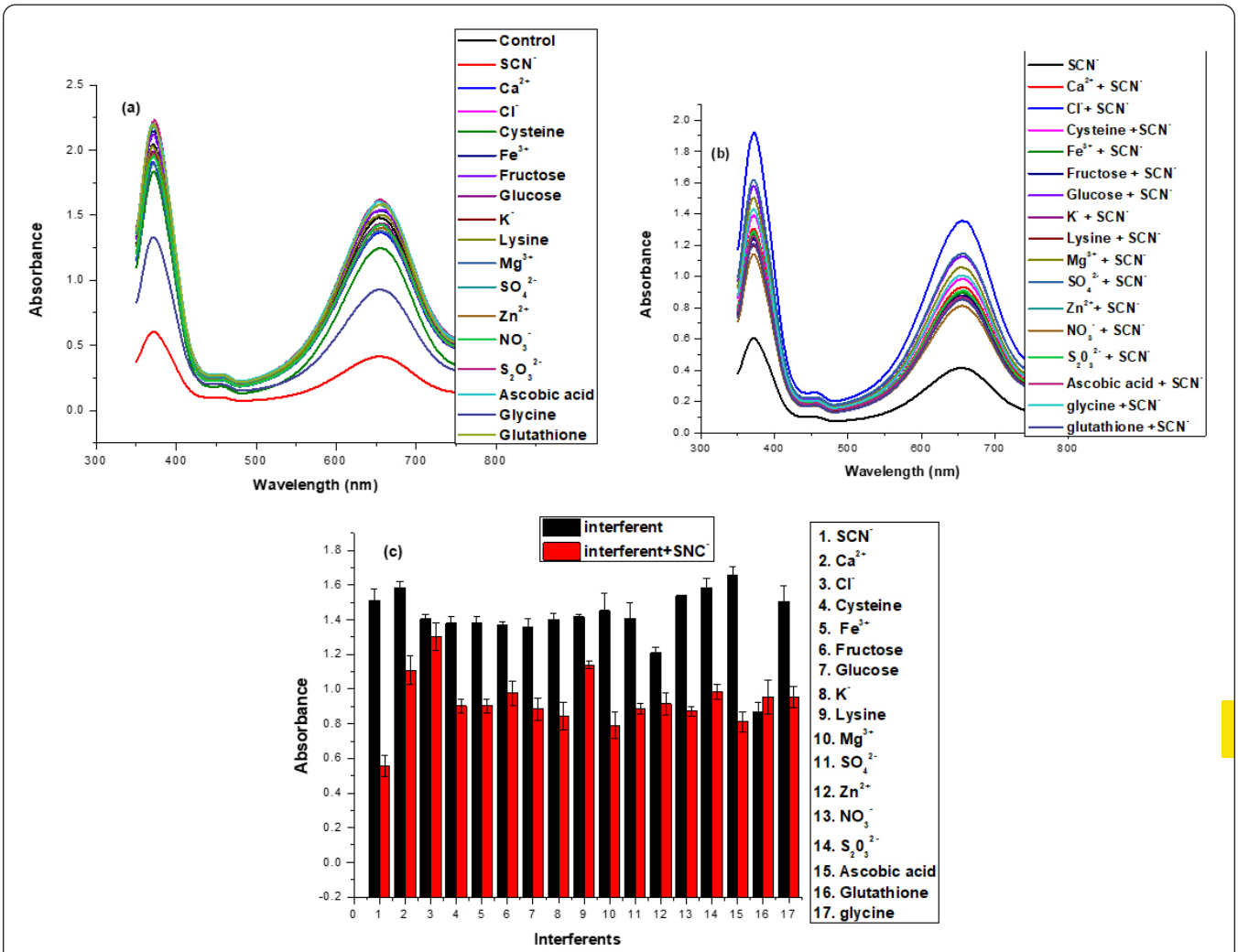


Figure 8: Selectivity if the AgNPs with oxidase-like property for determining SCN– a. UV vis spectra of systems containing TMB and potentially interfering species, b. UV vis spectra of systems containing TMB and SCN– in the presence of potentially interfering species c. bar graph showing absorbance intensities of the reaction solution in the presence of potentially interfering species.

ysis of SCN^- in milk samples with good recoveries. The proposed colorimetric method could present new understanding into a simple green method for synthesis the of oxidase mimetics with desired catalytic characteristics for the colorimetric detection of SCN^- compared to commonly employed peroxidase mimetics which use the destructive and unstable H_20_2.

Acknowledgements

Part of this work was supported by the Botswana International University of Science and Technology (BIUST), through the Office of Research, Development, and Innovation (ORDI).

Conflict of Interest

None.

References

1. Ahmed SR, Sherazee M, Srinivasan S, Rajabzadeh AR. 2022. Positively charged gold quantum dots: An nanozymatic "off-on" sensor for thiocyanate detection. *Foods* 11(9): 1189. https://doi.org/10.3390/foods11091189
2. Kanthale P, Kumar A, Upadhyay N, Lal D, Rathod G, et al. 2015. Qualitative test for the detection of extraneous thiocyanate in milk. *J Food Sci Technol* 52(3): 1698–1704. https://doi.org/10.1007/s13197-013-1174-9
3. Yong L, Wang Y, Yang D, Liu Z, Abernethy G, et al. 2017. Investigation of concentration of thiocyanate ion in raw cow's milk from china, new zealand and the netherlands. *Food Chem* 215: 61–66. https://doi.org/10.1016/j.foodchem.2016.07.130
4. Sharma S, Singh AK, Kaushik S, Sinha M, Singh PR, et al. 2013. Lactoperoxidase: structural insights into the function, ligand binding and inhibition. *Int J Biochem Mol Biol* 4(3): 108-128.
5. Seifu E, Buys EM, Donkin E. 2005. Significance of the lactoperoxidase system in the dairy industry and its potential applications: a review. *Trends Food Sci Technol* 16(4): 137–154. https://doi.org/10.1016/j.tifs.2004.11.002
6. Guidelines for the preservation of raw milk by use of the Lactoperoxidase system. [http://siweb1.dss.go.th/standard/Fulltext/codex/CXG_013E.pdf]
7. Song J, Huang PC, Wan YQ, Wu FY, 2016. Colorimetric detection of thiocyanate based on anti-aggregation of gold nanoparticles in the presence of cetyltrimethyl ammonium bromide. *Sens Actuators B Chem* 222: 790–796. https://doi.org/10.1016/j.snb.2015.09.006
8. Benefits and potential risks of the Lactoperoxidase system of raw milk preservation: report of an FAO/WHO technical meeting. [https://www.who.int/publications/i/item/9241594659] Accessed on December 24, 2022
9. Aklilu EG, Adem A, Kasirajan R, Ahmed Y. 2021. Artificial neural network and response surface methodology for modeling and optimization of activation of lactoperoxidase system. *S Afr J Chem Eng* 37: 12–22. https://doi.org/10.1016/j.sajce.2021.03.006
10. Fweja LWT, Lewis MJ, Grandison AS. 2007. Alternative strategies for activation of the natural lactoperoxidase system in cows' milk: trials in tanzania. *J Dairy Res* 74(4): 381–386. https://doi.org/10.1017/S0022029907002671
11. Lin X, Hasi WLJ, Lou XT, Lin S, Yang F, et al. Rapid and simple detection of sodium thiocyanate in milk using surface-enhanced raman spectroscopy based on silver aggregates. 45(2): 162–167. https://doi.org/10.1002/jrs.4436
12. Keyvanfard M, Alizad K, Elahian P. 2012. Determination of thiocyanate by kinetic spectrophotometric flow injection analysis. *J Chem* 2013: 147364. https://doi.org/10.1155/2013/147364
13. Akiyama H, Toida T, Sakai S, Amakura Y, Kondo K, et al. 2006. Determination of cyanide and thiocyanate in sugihiratake mushroom using hplc method with fluorometric detection. *J Health Sci* 52(1): 73–77. https://doi.org/10.1248/jhs.52.73
14. Afkhami A, Soltani-Felehgari F, Madrakian T. 2014. Highly sensitive and selective determination of thiocyanate using gold nanoparticles surface decorated multi-walled carbon nanotubes modified carbon paste electrode. *Sens Actuators B Chem* 196: 467–474. https://doi.org/10.1016/j.snb.2014.01.115
15. Demkowska I, Polkowska Z, Namiesnik J. 2008. Application of ion chromatography for the determination of inorganic ions, especially thiocyanates in human saliva samples as biomarkers of environmental tobacco smoke exposure. *J Chromatogr B Analyt Technol Biomed Life Sci* 875(2): 419–426. https://doi.org/10.1016/j.jchromb.2008.09.018
16. Tezcan F. 2018. A sample stacking-capillary electrophoresis method for simultaneous determination of nitrate and thiocyanate ions of ultra-heat-treated milk samples. *Turk J Chem* 42(4): 1184–1190. https://doi.org/10.3906/kim-1801-15
17. Song J, Wu FY, Wan YQ, Ma LH. 2015. Ultrasensitive turn- on fluorescent detection of trace thiocyanate based on fluorescence resonance energy transfer. *Talanta* 132: 619–624. https://doi.org/10.1016/j.talanta.2014.10.023
18. Wang X, Wang H, Guo L, Chen G, Kong R, et al. 2020. Colorimetric detection of Hg (ii) based on the gold amalgam-triggered reductase mimetic activity in aqueous solution by employing AuNP@ MOF nanoparticles. *Analyst* 145(4): 1362–1367. https://doi.org/10.1039/C9AN02615K
19. Ahmed SR, Sherazee M, Srinivasan S, Rajabzadeh AR. 2022. Nanozymatic detection of thiocyanate through accelerating the growth of ultra-small gold nanoparticles/graphene quantum dots hybrids. *Food Chem* 379: 132152. https://doi.org/10.1016/j.foodchem.2022.132152
20. Dong H, Fan Y, Zhang W, Gu N, Zhang Y. 2019. Catalytic mechanisms of nanozymes and their applications in biomedicine. *Bioconjug Chem* 30(5): 1273–1296. https://doi.org/10.1021/acs.bioconjchem.9b00171
21. Gao L, Zhuang J, Nie L, Zhang J, Zhang Y, et al. 2007. Intrinsic peroxidase- like activity of ferromagnetic nanoparticles. *Nat Nanotechnol* 2(9): 577–583. https://doi.org/10.1038/nnano.2007.260
22. Wu J, Wang X, Wang Q, Lou Z, Li S, et al. 2013. Nanomaterials with enzyme-like characteristics nanozymes: next- generation artificial enzymes (II). *Chem Soc Rev* 48: 1004-1076. https://doi.org/10.1039/C8CS00457A
23. Peng CF, Pan N, Zhi-Juan Q, Wei XL, Shao G. 2017. Colorimetric detection of thiocyanate based on inhibiting the catalytic activity of cystine-capped core-shell Au@ Pt nanocatalysts. *Talanta* 175: 114–120. https://doi.org/10.1016/j.talanta.2017.06.005
24. He Y, Niu X, Li L, Li X, Zhang W, et al. 2018. Microwave-assisted fabrication of bimetallic pdcu nanocorals with enhanced peroxidase-like activity and efficiency for thiocyanate sensing. *ACS Appl Nano Mater* 1(5): 2397–2405. https://doi.org/10.1021/acsanm.8b00578
25. Alula MT, Feke K. 2021. Peroxidase-like activity of silver nanoparticles loaded filter paper and its potential application for sensing. *J Clust Sci* in press. https://doi.org/10.1007/s10876-021-02202-5
26. Jin S, Wu C, Ye Z, Ying Y. 2019. Designed inorganic nanomaterials for intrinsic peroxidase mimics: a review. *Sens Actuators B Chem* 283: 18–34. https://doi.org/10.1016/j.snb.2018.10.040
27. Wang GL, Xu XF, Cao LH, He HC, Li JZ, et al. 2014. Mercury (II)-stimulated oxidase mimetic activity of silver nanoparticles as a sensitive and selective mercury (II) sensor. *Rsc Adv* 4(12): 5867–5872. https://doi.org/10.1039/C3RA45226C
28. Nyoni S, Muzenda E, Mukaratirwa-Muchanyereyi N. 2019. Characterization and evaluation of antibacterial activity of silver nanoparticles prepared from *Sclerocarya birrea* stem bark and leaf extracts. *Nano Biomed Eng* 11(1): 28–34. https://doi.org/10.5101/nbe.v11i1.p28-34

29. Jain D, Daima HK, Kachhwaha S, Kothari LS. 2009. Synthesis of plant-mediated silver nanoparticles using papaya fruit extract and evaluation of their anti-microbial activities. *Dig J Nanomater Biostruct* 4(3): 557–563.

30. Gregory M, Selvakesavan R, Franklin G, Sarmento B, Dias PCA. 2014. Green synthesis of silver nanoparticles using withania somnifera extract and their incorporation into a cream with antibacterial activity. *Planta Med* 80(16): SL26. https://doi.org/10.1055/s-0034-1394514

31. Bhagat M, Anand R, Datt R, Gupta V, Arya S. 2019. Green synthesis of silver nanoparticles using aqueous extract of rosa brunonii lindl and their morphological, biological and photocatalytic characterizations. *J Inorg Organomet Polym* 29(3): 1039–1047. https://doi.org/10.1007/s10904-018-0994-5

32. Some S, Sarkar B, Biswas K, Jana TK, Bhattacharjya D, et al. 2020. Biomolecule functionalized rapid one-pot green synthesis of silver nanoparticles and their efficacy toward the multidrug resistant (MDR) gut bacteria of silkworms (*Bombyx mori*). *RSC Adv* 10(38): 22742–22757. https://doi.org/10.1039/d0ra03451g

33. Busa LSA, Komatsu T, Mohammadi S, Maeki M, Ishida A, et al. 2016. 3, 3, 5, 5-tetramethylbenzidine oxidation on paper devices for horseradish peroxidase-based assays. *Anal Sci* 32(8): 815–818. https://doi.org/10.2116/analsci.32.815

34. Hu JW, Li JF, Ren B, Wu Deyin, Ren B, et al. 2007. Palladium-coated gold nanoparticles with a controlled shell thickness used as surface-enhanced Raman scattering substrate. *J Phys Chem C* 111(3): 1105–1112. https://doi.org/10.1021/jp0652906

35. Zhang Z, Zhang J, Qu C, Pan D, Chen Z, et al. 2012. Label free colorimetric sensing of thiocyanate based on inducing aggregation of tween 20-stabilized gold nanoparticles. *Analyst* 137(11): 2682–2686. https://doi.org/10.1039/C2AN35433K

36. Drozd M, Pietrzak M, Parzuchowski PG, Malinowska E. 2016. Pitfalls and capabilities of various hydrogen donors in evaluation of peroxidase-like activity of gold nanoparticles. *Anal Bioanal Chem* 408(29): 8505 8513. https://doi.org/10.1007/s00216-016-9976-z